Nonreciprocal Transport Reveals a Critical Boundary between Josephson and Pancake Vortex Dynamics

Peng Dong (董鹏),[1,2] Yanjiang Wang (王艳江),[1,2] Jianjun Xiao (肖建军),[1,2] Yang-Yang Lyu (吕阳阳),[3] Huabing Wang (王华兵),[3] Jinghui Wang (王靖珲),[1,2] Xiang Zhou (周翔),[1,2] Yueshen Wu (吴越珅),[1,2,*] Yulin Chen (陈宇林),[1,2,4] and Jun Li (李军)[1,2,†]

[1] *ShanghaiTech Laboratory for Topological Physics & School of Physical Science and Technology, ShanghaiTech University, Shanghai 201210, China*

[2] *State Key Laboratory of Quantum Functional Materials, ShanghaiTech University, Shanghai 201210, China*

[3] *School of Electronic Science and Engineering, Nanjing University, Nanjing 210023, China*

[4] *Department of Physics, Clarendon Laboratory, University of Oxford, Oxford OX1 3PU, United Kingdom*

(Dated: October 29, 2026)

Highly anisotropic superconductors host distinct vortex excitations whose roles in transport can be difficult to separate. In $Bi_2Sr_2CaCu_2O_{8+\delta}$, an in-plane magnetic field generates Josephson vortices between CuO_2 layers, whereas a finite out-of-plane field component nucleates pancake vortices in the superconducting planes. Although tilted magnetic fields are known to produce rich mixed vortex configurations, identifying which vortex subsystem dominates dissipation remains challenging with conventional transport. Here we show that nonreciprocal transport provides a symmetry-sensitive route to this problem in mechanically exfoliated $Bi_2Sr_2CaCu_2O_{8+\delta}$ flakes. Using second-harmonic transport under an ac current drive, we find a pronounced nonlinear response near T_c that flips sign upon reversing the in-plane magnetic field, while such sign-reversing nonreciprocal response is not resolved for out-of-plane fields. The nonlinear response is concentrated in the resistive superconducting transition region. We discuss its connection to Josephson-vortex dynamics qualitatively, using the field-orientation dependence and the competition between thermal fluctuations and pinning. Upon introducing a small out-of-plane tilt, the nonreciprocal signal abruptly collapses at a critical angle of about 2°–2.5°. The superconducting critical field also shows a rapid suppression when the field is tilted away from the *ab* plane, and its angular dependence remains broadly consistent with the anisotropic Ginzburg-Landau description. The much narrower collapse of the nonreciprocal response therefore cannot be attributed simply to an anomalous deviation of the superconducting critical field from conventional angular scaling. This sharp angular selectivity is consistent with a change in the vortex dynamics contributing to nonlinear transport and supports nonreciprocity as a symmetry-sensitive probe of vortex dynamics in mixed states.

Keywords: Nonreciprocal transport; Vortex dynamics; Cuprates; High temperature superconductors

Vortex dynamics in highly anisotropic superconductors is central to understanding dissipation, pinning, and phase coherence in the mixed state [1]. In layered cuprates, the strong anisotropy and weak interlayer coupling make vortex strongly dependent on field orientation rather than describable as a single conventional Abrikosov line. As illustrated in Fig. 1(a)–(c), a field component perpendicular to the CuO_2 planes generates pancake vortices in the superconducting layers, whereas an in-plane field produces Josephson vortices between adjacent layers; a tilted field can bring the two vortex subsystems into coexistence [2–6]. $Bi_2Sr_2CaCu_2O_{8+\delta}$ is an extreme example of this regime because its weak interlayer coupling makes the vortex configuration exceptionally sensitive to field orientation. Such tilted-field states provide a rich platform for studying vortex matter, while also leaving open the dynamical hierarchy that determines which vortex subsystem controls dissipative transport.

Extensive studies have clarified how Josephson and pancake vortices arrange in tilted magnetic fields. Theory predicts that the two field components generate crossing vortex lattices, vortex chains, and mixed chain-lattice states through the interaction between Josephson and pancake vortices [7–9]. Experiments using magnetization, conventional transport, and magnetic imaging have observed related melting anomalies, vortex-chain structures, composite-to-tilted-lattice transitions, and intertwined vortex configurations in Bi-2212 [6, 10–13]. These works established tilted fields as a powerful way to tune vortex configuration. However, when Josephson and pancake vortices coexist, conventional transport generally measures their combined dissipation and does not directly reveal which vortex mode dominates the transport response. Thus, the missing information is not the vortex configuration itself, but the dynamical hierarchy of vortex transport.

Nonreciprocal transport provides a possible route to this missing dynamical information because it is sensitive not only to dissipation, but also to the symmetry of the motion. For the field-odd magnetochiral response considered here, an applied magnetic field breaks time-

* wuysh@shanghaitech.edu.cn
† lijun3@shanghaitech.edu.cn

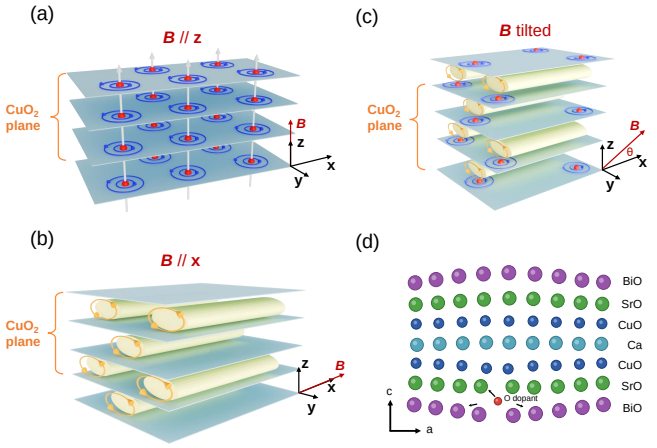

FIG. 1. Schematic of vortex configurations and local symmetry breaking in $Bi_2Sr_2CaCu_2O_{8+\delta}$. (a) For $H \parallel c$, pancake vortices form in the CuO_2 planes. Red represents the pancake vortex cores, blue indicates the circulating supercurrents, and white denotes the magnetic field lines penetrating the vortex cores. (b) For $H \parallel ab$, Josephson vortices are confined between adjacent superconducting layers. Yellow represents the Josephson vortices and their associated circulating currents. (c) Under a tilted magnetic field, Josephson and pancake vortices coexist in a crossing-vortex configuration, θ is the angle between the x-axis and the z-axis, marked by the red arrow. (d) Schematic of dopant-related local lattice distortion in the layered crystal, illustrating a local inversion-asymmetric component normal to the CuO_2 planes, along the c axis [14, 15].

reversal symmetry, while inversion asymmetry permits a direction-dependent nonlinear voltage. The leading contribution can be detected as an even-in-current response, $V = R_1 I + R_2 I^2 + \cdots$ [16, 17]. In the superconducting mixed state, such a response can arise when moving vortices experience direction-dependent depinning or mobility, as established in vortex ratchet systems, superconducting vortex diodes, and recent nonlinear Hall measurements of vortex motion [18, 19, 21**?**]. $Bi_2Sr_2CaCu_2O_{8+\delta}$ is especially relevant because nanoscale electronic inhomogeneity, structural supermodulation, and hidden spin-momentum locking indicate locally inversion-asymmetric environments [22–25]; the local symmetry-breaking direction associated with the layered structure is illustrated schematically in Fig. 1(d). Since Josephson and pancake vortices have distinct spatial structures and flow geometries, they may couple differently to such local symmetry breaking. This motivates using nonreciprocal transport to test whether different vortex-motion channels can be distinguished experimentally.

Here we experimentally test this possibility using second-harmonic transport in mechanically exfoliated $Bi_2Sr_2CaCu_2O_{8+\delta}$ flakes under angle-controlled magnetic fields. We use the first-harmonic resistance to distinguish the zero-resistance state, the superconducting transition, the fluctuation and normal state, and locate the second-harmonic response within these temperature ranges. A clear nonreciprocal response that reverses sign upon magnetic-field reversal is observed for an in-plane field perpendicular to the current, whereas no such component is resolved for an out-of-plane field. Introducing a small out-of-plane component sharply suppresses the signal within about 2°–2.5° of the sample plane. We discuss this selectivity in terms of Josephson-vortex-related dynamics and their modification by the perpendicular field component, without using a fitted transition temperature to assign a specific vortex-motion regime.

Thin Bi-2212 flakes were prepared by mechanical exfoliation in an Ar-filled glovebox with H_2O and O_2 levels below 0.01 ppm and transferred onto SiO_2/Si substrates. Special care was taken to minimize wrinkles, bubbles, trapped residues, and contact inhomogeneity during exfoliation, transfer, and contacting. These precautions reduce unintended device asymmetry while retaining the intrinsic local symmetry breaking of Bi-2212. Devices used for the present measurements were selected from flat and uniform flakes without visible bubbles or strongly strained regions. Electrical contacts were formed using silver conductive paste in a four-probe geometry. An optical image of a representative device in Fig. S1 and the measurement geometry are shown in Fig. 2(a).

Nonreciprocal transport was measured using a standard lock-in technique in a Quantum Design Physical Property Measurement System equipped with sample rotators for magnetic-field angle control. A sinusoidal current with amplitude I was applied along the device channel, and the first and second harmonic voltages (V_ω and $V_{2\omega}$) were recorded. We define

$$R_\omega = \frac{\sqrt{2}V_\omega}{I}, \qquad R_{2\omega} = \frac{\sqrt{2}V_{2\omega}}{I}, \tag{1}$$

where the factor of $\sqrt{2}$ follows the voltage-amplitude convention used in the lock-in analysis. The second-harmonic channel was phase-corrected by $\pi/2$ following the lock-in convention used in the measurement. The second-harmonic response detects the even-in-current component of the nonlinear voltage, $V = R_1 I + R_2 I^2 + \cdots$. In the superconducting mixed state, such a response can arise when moving vortices experience direction-dependent depinning, viscosity, or mobility in a locally inversion-asymmetric environment. The second-harmonic channel therefore provides a symmetry-sensitive probe of vortex motion.

We first characterize the superconducting transition and the temperature window in which the nonlinear signal is measured under a fixed in-plane magnetic field. The first-harmonic resistance $R_\omega(T)$ shows a sharp transition, as shown in Fig. 2(b), with an onset near 96.8 K and a zero-resistance temperature near 87 K in the representative device. We characterize the nonlinear-response window directly from the measured first- and second-harmonic resistances. In the finite-field mixed state of a type-II superconductor, thermally activated vortex motion, depinning, or melting can produce finite resistance while superconducting correlations persist [1]. Spatial

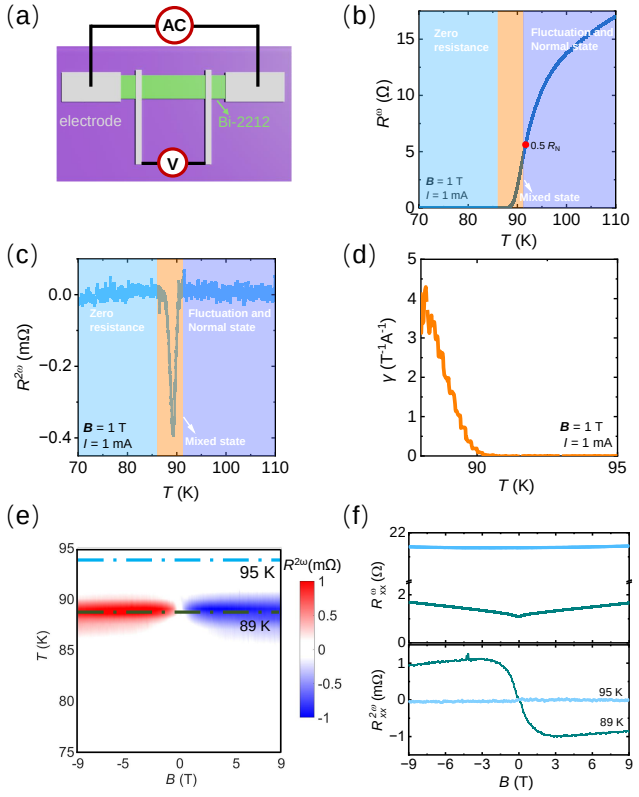

FIG. 2. Device geometry and nonreciprocal response. (a) The measurement geometry of the mechanically exfoliated $Bi_2Sr_2CaCu_2O_{8+\delta}$ device combined with the four-probe second-harmonic measurement geometry. (b) Temperature dependence of the measured first-harmonic resistance under an in-plane field of 1 T perpendicular to the current and an ac current of 1 mA, suggesting the zero-resistance state, the resistive superconducting transition, and the fluctuation and normal state. (c) Temperature dependence of the second-harmonic resistance, showing that the nonlinear response is concentrated in the resistive superconducting transition region. (d) Temperature dependence of the nonreciprocal coefficient extracted from the measured harmonics under the same field and current conditions. (e) Mapping of the second-harmonic resistance as a function of temperature and magnetic field. (f) First- and second-harmonic magnetoresistance at two representative temperatures (89 K and 95 K) selected from (e).

heterogeneity and thermal-history effects can also influence vortex behavior near the transition [26].

The corresponding second-harmonic resistance $R_{2\omega}(T)$ is shown in Fig. 2(c). The signal is concentrated in the resistive superconducting transition region and is strongly reduced outside this range. Its temperature dependence motivates a vortex-related interpretation, which we assess together with field symmetry, orientation dependence, and possible thermal contributions. Using the conventional magnetochiral normalization,

$$\gamma = \frac{2R_{2\omega}}{BIR_{\omega}}, \tag{2}$$

we extract the nonreciprocal transport coefficient as a function of temperature [Fig. 2(d)]. The resulting γ is of order 4 $\mathrm{A^{-1}T^{-1}}$ near the resistive transition. For comparison, gated superconducting MoS_2 exhibits $\gamma \approx 1200$ $\mathrm{A^{-1}T^{-1}}$ near T_c using the same second-harmonic normalization [16], about 300 times the value measured here. This comparison places the Bi-2212 response at a smaller device-level magnitude.

We further map the second-harmonic resistance as a function of temperature and magnetic field [Fig. 2(e)]. The raw data are shown in Fig.S2. Because the upper critical field of Bi-2212 is very large, the full mixed-state boundary cannot be accessed within the available magnetic-field range except near T_c. The nonreciprocal response is therefore studied in the near-T_c vortex-liquid regime, where mobile vortices dominate dissipation. Figure 2(f) compares the first- and second-harmonic magnetoresistance at two representative temperatures selected from the mapping, showing how the nonlinear response emerges within this vortex-flow window, with a clear odd-field symmetry characteristic of nonreciprocal transport.

We next examine the excitation-current dependence of the nonlinear response under an in-plane magnetic field. Figure 3(a) shows the second-harmonic resistance as a function of magnetic field for different ac current amplitudes. The signal preserves its odd-in-field character while growing systematically with current, confirming that the measured response belongs to the nonlinear transport channel rather than to a linear magnetoresistive background. The raw data are shown in Fig. S3. For the present measurement geometry, Eq. (2) implies the low-current scaling

$$R_{2\omega} = \frac{1}{2}\gamma BIR_{\omega}, \tag{3}$$

or equivalently $R_{2\omega} \propto BI$ when γ and R_{ω} are fixed. The magnitude of the second-harmonic resistance extracted from these traces is summarized in Fig. 3(b). In the low-current regime, the response shows an approximately linear dependence on current, consistent with a second-order voltage contribution because $V_{2\omega} \propto I^2$. At larger drive currents, deviations from this low-current scaling may reflect current-induced changes in vortex dynamics or heating. We therefore focus on the low-current regime for the field-orientation and angle-dependent measurements discussed below.

We also consider thermal-voltage mechanisms in this geometry. Contact Joule heating can generate an in-plane temperature gradient and a longitudinal Seebeck voltage, which is even under field reversal [27]. With current along x and in-plane field along y, a c-axis temperature gradient can instead generate a longitudinal Nernst voltage along x [28]. A stationary gradient produces a static voltage, which does not enter the second-harmonic lock-in channel. The sharp angular suppression further constrains an environmental thermal background that varies smoothly with orientation.

Bi-2212 exhibits an incommensurate structural super-

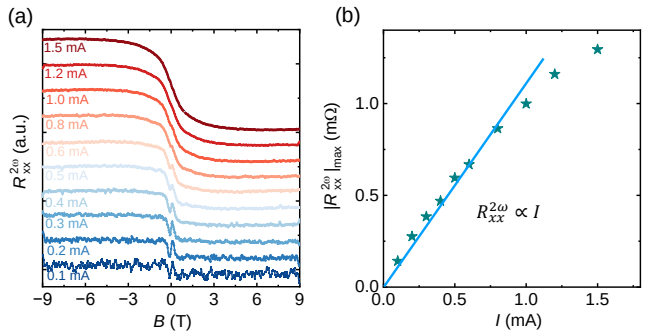

FIG. 3. Current dependence of the second-harmonic response at T = 89 K with the magnetic field applied perpendicular to the current ($B \perp I$). (a) Second-harmonic resistance $R_{2\omega}$ as a function of magnetic field under different ac current amplitudes. (b) Magnitude of the second-harmonic resistance extracted from (a) as a function of current amplitude. The approximately linear behavior at low current is consistent with a second-order nonlinear voltage response.

modulation and dopant-related local lattice distortions. Imaging of interstitial oxygen reveals changes in local structure and charge transfer between the BiO and CuO_2 planes [14], while strain associated with the supermodulation correlates with the distribution of certain oxygen defects [15]. A dopant on one side of a CuO_2 plane can make its two sides locally inequivalent, providing an inversion-asymmetric component along the c axis. Spin-resolved ARPES and bilayer spin-orbit models provide complementary evidence and a theoretical description of local out-of-plane asymmetry [25, 29, 30].

Local inversion asymmetry can coexist with a globally centrosymmetric crystal and does not by itself ensure a macroscopic nonreciprocal charge response. A net signal requires unequal contributions from inversion-related local environments. Dopant-induced variations in the local potential, interlayer coupling, and pinning could make these environments contribute unequally along active vortex-transport paths. A residual imbalance is qualitatively compatible with the small net nonlinear response, but its microscopic origin is not determined by the measured coefficient. We consider this a possible link between local c-axis asymmetry and the observed field-odd response.

We then use magnetic-field orientation to test whether the nonreciprocal signal is a generic consequence of vortex flow or is selective to a particular vortex-motion channel. Figure 4(a) shows the field dependence of second-harmonic resistances under an out-of-plane magnetic field, $B \parallel c$ and an in plane magnetic field , $B \perp I$. The first-harmonic resistance in Fig. S2 exhibits the expected field-broadened superconducting transition, indicating that the out-of-plane field introduces mobile pancake vortices near T_c. In contrast, the second-harmonic resistance remains negligible over the same temperature range. Thus, pancake-vortex-dominated transport produces ordinary dissipative flux flow but does not generate a measurable nonreciprocal response in our devices. This field-orientation contrast indicates the key mode selectivity of the measurement: the second-harmonic channel does not simply track the total vortex dissipation, but selectively highlights vortex motion that couples to local inversion-symmetry breaking.

We next fix the temperature and magnetic-field magnitude and rotate the field away from the sample plane. Figure 4(b) compares the angular dependence of the first- and second-harmonic resistances. The first-harmonic resistance evolves smoothly with field angle, reflecting the continuous change in the total vortex dissipation. By contrast, the second-harmonic resistance is confined to a narrow angular window around the in-plane field direction. A magnified view near the in-plane orientation [lower panel of Fig. 4(b)] shows that the nonreciprocal signal collapses once the field is tilted by only about 2.5°. This sharp angular selectivity indicates that the second-harmonic signal is not governed by the total vortex density, but by the dominant vortex-transport mode. A similar odd-field second-harmonic response, along with a sharp angular dependence, is also observed in the bulk sample (see Figs. S5–S8), consistent with the findings in the exfoliated flake.

To exclude the possibility that this angular threshold is an artifact of the particular magnetic-field magnitude chosen in the angle scan, or of the strongly anisotropic upper critical field, we performed field sweeps at several fixed angles near the in-plane direction. As shown in Fig. 4(c), angles labeled a–i were selected around 180°, and the second-harmonic magnetoresistance was measured as a function of magnetic field at each angle [Fig. 4(d)]. The nonreciprocal response appears only for angles within the same narrow in-plane window and remains absent outside it over the accessible field range. This supports the view that the collapse of the second-harmonic signal is controlled primarily by field orientation rather than by a specific value of the applied magnetic field. The sharp orientation dependence is consistent with the known sensitivity of Bi-2212 crossing-vortex and vortex-chain structures to a small out-of-plane component [6, 8, 12]. The disappearance of nonreciprocity therefore indicates a switching of the dominant vortex-transport mode, from Josephson-vortex-dominated motion near the in-plane direction to pancake-vortex-dominated motion once a small perpendicular component is introduced.

The same angular region is also reflected in the conventional resistive transition. From the field-sweep data, we extracted a superconducting critical field using the criterion $R = 1.5\ \Omega$ and plotted its angular dependence in Fig. 4(e). The raw data are showed in Fig. S4. The critical field is strongly enhanced near the ab plane and decreases rapidly as the field is tilted away from the plane. Within the experimental angular range, this resistively defined critical field does not show a clear deviation from the anisotropic Ginzburg-Landau angular dependence, and it is also comparable to the sharp cusp expected

in the two-dimensional Tinkham form near the parallel-field direction [31, 32]. Thus, the disappearance of the second-harmonic signal should not be interpreted as arising from an unconventional angular dependence of the superconducting critical field itself. Rather, because the nonreciprocal response vanishes while the conventional critical-field evolution remains compatible with standard anisotropic superconducting scaling, the data indicate that the nonlinear signal is controlled by the dominant vortex-motion channel. A small perpendicular component can nucleate pancake vortices and couple them to the Josephson-vortex structure, switching the transport response away from the near-in-plane Josephson-vortex regime without requiring a breakdown of the conventional Ginzburg-Landau critical-field description.

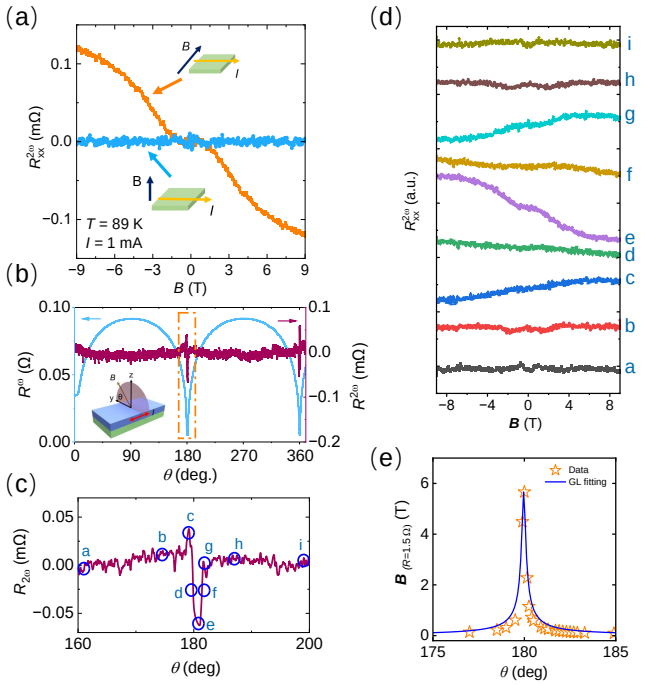

FIG. 4. Field-orientation dependence and critical switching of vortex transport modes. (a) Field dependence of second-harmonic resistances under a perpendicular magnetic field, $B \parallel c$ and an in plane magnetic field , $B \perp I$, showing no resolved field-odd second-harmonic response for $B \parallel c$. (b) Angular dependence of the first- and second-harmonic resistances at fixed temperature (T= 89 K) and magnetic-field magnitude(B= 9 T). The upper panel shows the full angular dependence, while the lower panel magnifies the region near the in-plane field direction and reveals that the nonreciprocal signal survives only within about 2.5°. (c) Zoom-in view of the region near 180 in (b), and selected angles a–i near 180° used for the field-sweep measurements. (d) Second-harmonic magnetoresistance measured at these selected angles. The field-odd response is resolved only within the narrow near-in-plane angular range over the accessible field interval. (e) Angular dependence of the superconducting critical field extracted using the $R = 1.5\ \Omega$ resistance criterion, with the inset magnifying the near-in-plane angular range.

Our interpretation follows the qualitative vortex dynamics of a type-II superconductor near its finite-field resistive transition. Near the transition, thermal energy increases smoothly, whereas the superfluid stiffness, condensation energy, and interlayer Josephson coupling weaken. The associated reduction in vortex-energy scales and fluctuation-induced softening of effective layer pinning may make cross-layer JV motion more accessible [33, 34]. For current along x, in-plane field along y, and the c axis along z, the Lorentz force is along z. A JV flux-motion contribution to the longitudinal voltage requires a c-axis velocity component, since $\mathbf{E} = \mathbf{B} \times \mathbf{v}$ gives $E_x = B_y v_c$. Thermally excited kinks or local phase rearrangements may allow current-biased transfer of JV segments between neighboring interlayer regions.

The cross-layer motion of JV segments can produce phase slips: the associated rearrangement of the interlayer phase changes the superconducting phase difference along the voltage-measurement path. A finite average voltage results when the current biases these JV-motion-induced phase slips so that forward and backward events occur at unequal rates [34, 35]. A theoretical smectic vortex state under strong parallel fields provides a related setting for collective phase relaxation and KT-type behavior [36]. Hu and Tachiki also found a possible KT-type intermediate phase above a multicritical field in a highly anisotropic parallel-field JV system [33].

A perpendicular field component introduces pancake vortices that can interact with, drag, or pin the JV structure [6–10, 12]. Such coupling provides a possible explanation for the sharp suppression of the field-odd response upon tilting. The contributions of the two vortex subsystems can be described phenomenologically by $\gamma_{\rm eff} \simeq w_J\gamma_J + w_P\gamma_P$, where w_J and w_P denote their respective fractions of the linear vortex-flow resistance, with $w_J + w_P = 1$, and γ_J and γ_P are their effective nonlinear coefficients in the measurement geometry. Near the in-plane direction, JV motion couples to the local c-axis asymmetry and supplies the dominant nonreciprocal contribution. Pancake-vortex motion contributes to the linear dissipation but produces little detectable second-harmonic response for an out-of-plane field. Upon tilting, the crossing interaction can impede JV motion and shift the relative dissipative weight toward pancake vortices. In this picture, a reduction of the JV contribution suppresses the nonlinear signal even while the total resistance evolves smoothly. The sharp angular suppression thus reflects a redistribution of the two vortex contributions rather than simply a change in the total vortex density.

A field-free superconducting diode effect, characterized by unequal critical currents for opposite current directions, has been reported in Bi-2212 flakes, with rectification demonstrated up to 72 K [37]. Here we measure a field-odd second-harmonic response in the resistive transition region under a finite in-plane field, with representative angular measurements at 89 K. The different observables and measurement regimes mean that the two

findings are not mutually exclusive. The two phenomena involve distinct proposed mechanisms: Qi et al. associate the field-free diode effect with possible loop-current order and spontaneous time-reversal-symmetry breaking, whereas the present finite-field response is interpreted in terms of dissipative JV motion coupled to local inversion asymmetry, with time-reversal symmetry broken by the applied field.

We have shown that nonreciprocal transport provides a mode-selective probe of vortex dynamics in $Bi_2Sr_2CaCu_2O_{8+\delta}$. The second-harmonic response appears in the vortex-motion regime for in-plane magnetic fields, is consistent with the phenomenology of nonreciprocal superconducting transport, and is absent for perpendicular fields where pancake vortices dominate the flux-flow response. This field-orientation selectivity shows that the nonlinear signal is not a generic measure of vortex dissipation, but is associated with Josephson-vortex-dominated transport coupled to local inversion-symmetry breaking. By rotating the magnetic field away from the layers, we find that the nonreciprocal signal collapses within a small critical angle of about 2°-2.5°, indicating a switching of the dominant transport mode from Josephson-vortex motion to pancake-vortex motion. The resistively defined superconducting critical field decreases rapidly away from the in-plane direction but remains broadly compatible with the anisotropic Ginzburg-Landau angular dependence, showing that the collapse of nonreciprocity is not driven by an anomalous critical-field scaling. These results point to a critical boundary between two vortex transport regimes and introduce nonreciprocal transport as a symmetry-sensitive method for studying vortex dynamics in highly anisotropic superconductors.

ACKNOWLEDGMENTS

This work was supported by the National Key Projects for Research and Development of China (Grants No. 2022YFA1603903), the National Natural Science Foundation of China (Grants No. 62571327, 92565112, 92565305, 12434005, 12225407), Natural Science Foundation of Shanghai (Grants No. 25ZR1402374, 25ZR1402368, and 25ZR1401252), the Science and Technology Commission of Shanghai Municipality, the Shanghai Leading Talent Program of Eastern Talent Plan, State Key Laboratory of Micro-nano Engineering Science (Grant No. MES202603), and the Double First-Class Initiative Fund of ShanghaiTech University. Growth of hexagonal boron nitride crystals was supported by the Elemental Strategy Initiative conducted by the MEXT, Japan, Grant Number JPMXP0112101001, JSPS KAKENHI Grant Number JP20H00354 and A3 Foresight by JSPS.

DATA AVAILABILITY

The data that support the findings of this study are available from the corresponding author upon reasonable request.

[1] Blatter G, Feigel' man M V, Geshkenbein V B, Larkin A I, and Vinokur V M 1994 *Rev. Mod. Phys.* **66** 1125
[2] Clem J R 1991 *Phys. Rev. B* **43** 7837
[3] Bulaevskii L N, Ledvij M, and Kogan V G 1992 *Phys. Rev. B* **46** 366
[4] Grigorieva I V, Steeds J W, Balakrishnan G, and Paul D M 1995 *Phys. Rev. B* **51** 3765
[5] Vlasko-Vlasov V K, Welp U, Crabtree G W, Nikitenko V I, Benseman T M, and Kwok W K 2002 *Phys. Rev. B* **66** 014523
[6] Curran P J, Mohammed H A, Bending S J, Koshelev A E, Tsuchiya Y, and Tamegai T 2018 *Sci. Rep.* **8** 10914
[7] Koshelev A E 1999 *Phys. Rev. Lett.* **83** 187
[8] Koshelev A E 2005 *Phys. Rev. B* **71** 174507
[9] Buzdin A and Baladie I 2002 *Phys. Rev. Lett.* **88** 147002
[10] Grigorenko A N, Bending S J, Koshelev A E, Clem J R, Tamegai T, and Ooi S 2002 *Phys. Rev. Lett.* **89** 217003
[11] Koshelev A E, Buzdin A, Kakeya I, Kadowaki K, and Yamamoto T 2011 *Phys. Rev. B* **83** 224515
[12] Konczykowski M, van der Beek C J, Colson D, Bulaevskii L N, Geshkenbein V B, and Blatter G 2006 *Phys. Rev. Lett.* **97** 237005
[13] Correa A, Putilov A V, Plastovets V, Latyshev Y I, and Bending S J 2019 *Commun. Phys.* **2** 31
[14] Song D S, Zhang X F, Lian C S, Liu H, Alexandrou I, Lazic I, Bosch E G T, Zhang D, Wang L L, Yu R, Cheng Z Y, Song C L, Ma X C, Duan W H, Xue Q K, and Zhu J 2019 *Adv. Funct. Mater.* **29** 1903843
[15] Zeljkovic I, Nieminen J, Huang D, Chang T R, He Y, Jeng H T, Xu Z, Wen J, Gu G, Lin H, Markiewicz R S, Bansil A, and Hoffman J E 2014 *Nano Lett.* **14** 6749
[16] Wakatsuki R, Saito Y, Hoshino S, Itahashi Y M, Ideue T, Ezawa M, Iwasa Y, and Nagaosa N 2017 *Sci. Adv.* **3** e1602390
[17] Hoshino S, Wakatsuki R, Hamamoto K, and Nagaosa N 2018 *Phys. Rev. B* **98** 054510
[18] Villegas J E, Savel' ev S, Nori F, Gonzalez E M, Anguita J V, Garcia R, and Vicent J L 2003 *Science* **302** 1188
[19] Itahashi Y M, Ideue T, Saito Y, Shimizu S, Ouchi T, Nojima T, and Iwasa Y 2020 *Sci. Adv.* **6** eaay9120
[20] Gutfreund A, Matsuki H, Plastovets V, Noah A, Gorzawski L, Fridman N, Yang G, Buzdin A, Millo O, Robinson J W A, and Anahory Y 2023 *Nat. Commun.* **14** 1630
[21] Hashimoto M, Konoike T, Kobayashi T, Hoshino S, Kawada T, Yokouchi S, Uji S, Maeda A, and Shiomi Y 2025 *Phys. Rev. Lett.* **135** 136001
[22] Pan S H, O' Neal J P, Badzey R L, Chamon C, Ding H, Engelbrecht J R, Wang Z, Eisaki H, Uchida S, Gupta A K, Ng K-W, Hudson E W, Lang K M, and Davis J C 2001 *Nature* **413** 282
[23] Lang K M, Madhavan V, Hoffman J E, Hudson E W, Eisaki H, Uchida S, and Davis J C 2002 *Nature* **415** 412

[24] Andersen B M, Hirschfeld P J, and Slezak J A 2007 *Phys. Rev. B* **76** 020507
[25] Gotlieb K, Lin C-Y, Serbyn M, Zhang W, Smallwood C L, Jozwiak C, Eisaki H, Hussain Z, Vishwanath A, and Lanzara A 2018 *Science* **362** 1271
[26] Jayaram S, Lenger M, Zhao D, Pupim L, Taniguchi T, Watanabe K, Peng R, Scheffler M, Stöhr R, Scheurer M S, Smet J H, and Wrachtrup J 2025 *Phys. Rev. Lett.* **135** 126001
[27] Nagata U, Aoki M, Daido A, Kasahara S, Kasahara Y, Ohshima R, Ando Y, Yanase Y, Matsuda Y, and Shiraishi M 2025 *Phys. Rev. Lett.* **134** 236703
[28] Behnia K and Aubin H 2016 *Rep. Prog. Phys.* **79** 046502
[29] Liu W J, Zha H M, Gu G-D, Shen X P, Ye M, and Qiao S 2023 *Chin. Phys. Lett.* **40** 037402
[30] Raines Z M, Allocca A A, and Galitski V M 2019 *Phys. Rev. B* **100** 224512
[31] Tinkham M 1963 *Phys. Rev.* **129** 2413
[32] Mineev V P 2001 *Phys. Rev. B* **65** 012508
[33] Hu X and Tachiki M 2004 *Phys. Rev. B* **70** 064506
[34] Koshelev A E and Dodgson M J W 2013 *J. Exp. Theor. Phys.* **117** 449
[35] Halperin B I, Refael G, and Demler E 2010 *International Journal of Modern Physics B* **24** 4039
[36] Blatter G, Ivlev B I, and Rhyner J 1991 *Phys. Rev. Lett.* **66** 2392
[37] Qi S C, Ge J, Ji C C, Ai Y W, Ma G X, Wang Z Q, Cui Z H, Liu Y, Wang Q, and Wang J 2025 *Nat. Commun.* **16** 531